Polymer Bulletin (2020) 77:2205–2226
https://doi.org/10.1007/s00289-019-02856-2

ORIGINAL PAPER

Tetraphenylthiophene–thiazole-based π-conjugated polyazomethines: synthesis, characterization and gas sensing application

Y. S. Patil[1] · P. H. Salunkhe[1] · Y. H. Navale[2] · V. B. Patil[2] · V. P. Ubale[3] · A. A. Ghanwat[1]

Received: 10 December 2018 / Revised: 7 May 2019 / Accepted: 19 June 2019 / Published online: 21 June 2019
© Springer-Verlag GmbH Germany, part of Springer Nature 2019

Abstract

2,5-Bis(4-(2-aminothiazole) phenyl)-3 and 4-diphenyltetraphenyl thiophene (TPTPThDA) are fine processed in three steps. A series of polyazomethines containing thiophene–thiazole unit have been incorporated by the polycondensation of a new diamine, i.e. TPTPThDA, with proportionate of aromatic dialdehydes. The impact of insertion of thiazole entity in the polyazomethine matrix with the azo linkages having dialdehydes [isophthalaldehyde (1,3 IPA) and terephthalaldehyde (1,4 TPA)], on conductivity and gas sensing properties, has been studied. In all polyazomethines synthesized (PAM-01 to PAM-05), the preeminent in terms of conductivity and gas sensing properties has been established to be the PAM-03 containing polyazomethine matrix composition of 1,3 IPA and 1,4 TPA with thiophene–thiazole unit. After the infusion with the dialdehyde comonomers, an inflation of the molecular weight and the polyazomethines films were highly selective towards H_2S gas at 35 °C with great sensitivity and acceptable selectivity. Along this, all polyazomethines have T_g in the range of 257–260 °C and $T_{10\%}$ value of all thermally stable polyazomethines in air and nitrogen was in between of 458–545 °C and 527–601 °C, respectively. The polymer backbone contains rigid framework expect PAM-05, and due to this, they show less solubility in organic solvents. XRD study confirms that all the polyazomethines are amorphous in nature having broad peak in the range of 20°. The UV at 342 nm shows that there is a formation of imine (–C=N–) linkages in the polymer matrix which is helpful for the conduction of electron throughout. The band gap energy of PAM-3 is found as 3.63 eV.

✉ A. A. Ghanwat
anil_ghanwat@yahoo.com

[1] Polymer Research Laboratory, School of Chemical Sciences, Solapur University, Solapur, MS, India

[2] Functional Material Research Laboratory, School of Physical Sciences, Solapur University, Solapur, MS, India

[3] Department of Chemistry, DBF Dayanand College of Arts and Science, Solapur, MS, India

Keywords Polyazomethine · Thiophene–thiazole · Copolymer · Gas sensing · XRD

Introduction

Conjugated polyazomethines (PAMs) that incorporated divergent aromatic component in polymer framework having assorted bulky or pendant crowd with heterocyclic unit have been groomed and worn to explore the accoutrements of molecular building on electronic and optoelectronic material goods of conjugated polymers. These polymers are recognized as very important standing and applied class of conducting material for electronics and optoelectronics devices. Gas sensors gave a leading role in different fields such as environment monitoring, industrial harmful process control and also in various biological fields [1–5]. Recently conjugated and conducting material containing polymer gave a strong attention in the development and designing of dependable and supremely sensitive gas sensors [6, 7]. For the synthesis of immense performance portable gas sensors conducting polymer built-up and showing properties such as outstanding electrical properties, hasty preparation, resilience, small weight, and little power consumption [8–10]. In specific, synthesis of the conjugated and conducting material shows conductivity in polymer backbone. This type of conducting polymer can be synthesized by chemical or electrochemical adulterate/de-adulterate routes and follows the synthetic conditions. Gas sensors are designed with conductive and conjugated polymers functioning at low temperature or room temperature, for example, synthesized gas sensors have the superiority above the metal-based gas sensors [11, 12]. Aromatic polyazomethines contain azo group (–C=N–) in their backbone. This azo group replaces to their polyvinylene equivalents and isoelectronic material with owned carbon correspondents [12, 13]. More correctly, PAMs are efficiently incorporated by means of a simple difunctional molecule condensation reaction with production of neutral lighter molecules as the only outgrowth without any use of catalyst [14]. This synthetic route of polymers gave application in organic electronics because of the catalyst hindering in the main core of polymer matrix which alters their properties [15, 16]. The polymer can be refined by way of long-established method (easily by wiped-off superfluous precursor). This is due to the polymer backbone that contains only azo linkage functions and not the interfering impurities of metal, monomers and others [17–19]. The detail studies of azo compound started in 1923, and the corresponding polymers, i.e. polyazomethines, were begun in the year of 1950 [12, 20–23]. Conjugated polymers are composed of five-membered heterocyclic moieties in regard to good properties for advancement of device fabrication [24–29]. Alternatively, if satisfactory with constructing or designing and synthesis of the polymer backbone for conductive, the increase level of conduction by insertion of thiazole groups can be used with tetraphenylthiophene. PAMs containing 1,3 IPA or 1,4 TPA-substituted tetraphenyl thiophene–thaizole units have been perfectly largely symphonized displaying authentic electronic attribute confer to owned chemical essence and interlinked in a polymer framework, such as a great electricity or else an excellent gas sensing, and the literature is rare on thiophene–thiazole-built PAMs [30].

In this current research paper, we synthesized various tetraphenylthiophene–thiazole-based conjugated polyazomethines with thaizole ring unit special effects active nucleus for electron carrier condensing with a 1,3 IPA and 1,4 TPA aromatic ring units specialty for the gas sensing applications. Synthesized copolymers (PAM-03) of approximately 100 mg in 1 mL formic acid casted thin film on glass plate composed of 1,3 IPA, 1,4 TPA and thiophene–thiazole unit. The gas sensing achievement was deliberated for numerous oxidizing and reducing types of gases at 35 °C. Further gas detecting measurements, such as response, recovery times and selectivity, were similarly inspected as well as analysed.

Experimental section

Materials

Isophthalaldehyde (1,3 IPA), thiourea, terephthalaldehyde (1,4 TPA), sulphur powder, acetyl chloride, Br_2 solution and $AlCl_3$ were supplied by either Sigma-Aldrich or s d fine. *N*,*N*′-Dimethyl foramide (DMF, s d fine) and *N*,*N*′-dimethyl acetamide (DMAc, s d fine) were dried over P_2O_5, distilled under reduced pressure and kept over 4 Å molecular sieves. Solvents such as THF, DCM, methanol, ethanol and glacial acetic acid, were worn as collected. LiCl was dehydrated at 180 °C in vacuum oven for 14 h. Terahydrofuran (THF) and dichloromethane (DCM) were conserved by NaH and CaH_2 correspondingly afore procedure.

Instruments and measurements

The PAMs thin films were plunked onto glass substrate by adopting spin-coating technique. Fourier transform infrared (FTIR) spectrometry (Thermo Nicolet iS-10 Mid Fourier transform infrared between wave numbers of 650–4000 cm^{-1}) was engaged to classify the functional groups of precursor and polymers. The ^{1}H-NMR scan was operated on 400 MHz Bruker spectrometer in dimethyl sulfoxide-d6. Molecular weight of monomer is confirmed by MASS spectrometer. Ultraviolet–visible (UV–Vis) spectra were operated on a Beckman DU-640 spectrometer. The XRD analysis was drifting out by using X-ray diffractometer (ULTIMA IV Goniometer). Surface morphology of PAMs was done by scanning electron microscopy (SEM JEOL JSM-6360) instrument. Inherent viscosities of the PAMs were deliberate by an Ubbelohde suspended-level viscometer. Thermal behaviour of the PAMs was reconnoitred by a TGA—Mettler Toledo with pure nitrogen with stream amount of 20 ml/min and at a heating degree of 10 °C/min. Differential scanning calorimetry result was carried out on a Mettler Toledo DSC-1 STARe instrument to define the material softness or glass transition temperature of PAMs.

The silver connections were engraved on the exterior of the PAMs film and two probes were pined on the PAMs film by fixing their spot in the system. The temperature dependence electrical conductivity quantification of the PAMs was

accomplished through four-point probe system making use of 6-digit Keithley 6514 electrometer.

The PAMs sensor was operated at various temperatures towards numerous gases to achieve the constant resistance (R_a) with H_2S gas introduced keen on the object compartment and the sensor resistance touches the fresh persistent value (R_g). The H_2S gas response is calculated as

$$S(\%) = \frac{R_a - R_g}{R_a} \times 100 \quad (1)$$

where R_g is the sensor resistance dignified in the existence of the object gas and R_a in air. Response and recovery times are demarcated as the time desirable to touch 90% of the whole resistance alteration on disclosure to gas and air, respectively.

Synthesis

Monomer synthesis

2,5-Bis(4-(1-bromo) acetyl phenyl)-3,4-diphenyl thiophene (TPTPDAcBr)

Into 500-mL three-neck round-bottom flask, suspend 4.72 g (10 mmol) of diketone compound (TPTPDAc) in 200 mL glacial acetic acid and warm quietly till a transparent solution outcome. Then, 3.199 g (1 mL 20 mmol) of bromine was added dropwise, and the reaction flask was stirred at same temperature for 2 h. Then, cool and filter the crude product. It is washed with cold glacial acetic acid and then by small quantity of water and recrystallized with rectified spirit. Yield 79%, mp: 224–226 °C.

2,5-Bis(4-(2-aminothiazole) phenyl)-3,4-diphenyl thiophene (TPTPThDA)

Into 100-mL single-neck round-bottom flask, a mixture of TPTPDAcBr (5.6 g, 8.88 mmol) and thiourea (2.24 g, 29.47 mmol) was dissolved in 60 mL THF. The mixture was stirred and refluxed for 24 h. Then, cool the clear solution, transfer it to another beaker containing cold sodium acetate solution and stir it for 3 h. The crude product was filtered, washed by water and recrystallized with ethyl acetate as yellowish crystals. Yield 75%, mp: 236–238 °C.

Polymer synthesis

Synthesis of polyazomethines/co-polyazomethines (PAM-01 to PAM-05)

Into 100-mL three-neck round-bottom flask, a mixture of 0.584 g (TPTPThDA, 1 mmol) of diamine and 3 mL of dry DMAc was stirred under nitrogen gas to get transparent solution of diamine. Then, 0.134 g of dialdehyde (TPA/IPA/TPA + IPA,

1 mmol) was added to the above solution with constant stirring at room temperature and stirred for overnight in N_2 atmosphere. The mixture was reheated at 140 °C for 4 h. On cooling, the polymer mixture was gradually poured into water while continuing stirring, and precipitate of the resulting polymer was filtered off. Rinse with water and resulting brown product was obtained in high yield. Dry under vacuum at 80 °C for 8 h, to produce PAMs. By applying same procedure, all other PAMs are prepared in 93–100% yields.

Results and discussion

Monomer synthesis and characterization

The diamine precursor containing thiophene–thiazole unit (TPTPThDA) was synthesized in four steps, as sketched in Scheme 1. First step executes cylcocondensation of benzyl chloride and sulphur to yield 2,3,4,5 tetraphenylthiophene (TPTP). In the second step, the diketone compound (TPTPDAc) was obtained by direct acylation TPTP [31, 32]. The third step involved is bromination of TPTPDAc to give alpha-bromo derivative, i.e. TPTPDAcBr. In the fourth step, TPTPDAcBr undergoes ring closure with thiourea to give 2,5-bis(4-(2-aminothiazole) phenyl)-3,4-diphenyl thiophene (TPTPThDA). Chemical elucidation of new diamine precursor (TPTPThDA) was confirmed by proton-NMR, FTIR and mass spectral analysis.

The proton-NMR spectra of TPTPThDA are shown in Fig. 1. The resonance peak at 4.0 δ ppm (4 H) appears as singlet correlate to $–NH_2$ protons of the thiazole ring components. The resonance peak in the range of 6.4–7.6 δ ppm (16H) is for hetro-aromatic protons of tetraphenylthiophene–thiazole moiety. ^{1}H NMR analysis clearly indicated that diketone structure is completely transformed into diamine structure by cyclization. It has been also reported that ketonic methyl units of TPTPDAc are highly conjugated (enol form) with phenyl rings of TPTP and finally transformed into thaizole ring units. The FTIR spectrum of the corresponding diamine monomer (TPTPThDA) also supported the evidences of the successful achievement of complete ring cyclization of thaizole monomer, as shown in Fig. 2. The infrared spectrum showed absorption bands at 3400–3150 cm^{-1} ($–NH_2$ stretch). The mass spectrum shown in Fig. 3 was compatible by the true structure at m/e 584 related to the M^+ ion of TPTPThDA. The other disintegration pattern at m/e 555,537 and 385 proves the losing of 2-aminothiazole units.

Polymer synthesis and characterization

As presented in Scheme 2, a series of five new PAMs was prepared from new diamine precursor, i.e. 2,5-bis(4-(2-aminothiazole) phenyl)-3,4-diphenyl thiophene (TPTPThDA) with two different dialdehydes (IPA and TPA or varying mole ratio of IPA + TPA) by a high-temperature solution polycondensation method [33]. Yields and inherent viscosities are shown in Table 1. The synthesised PAMs were proved by FTIR spectra.

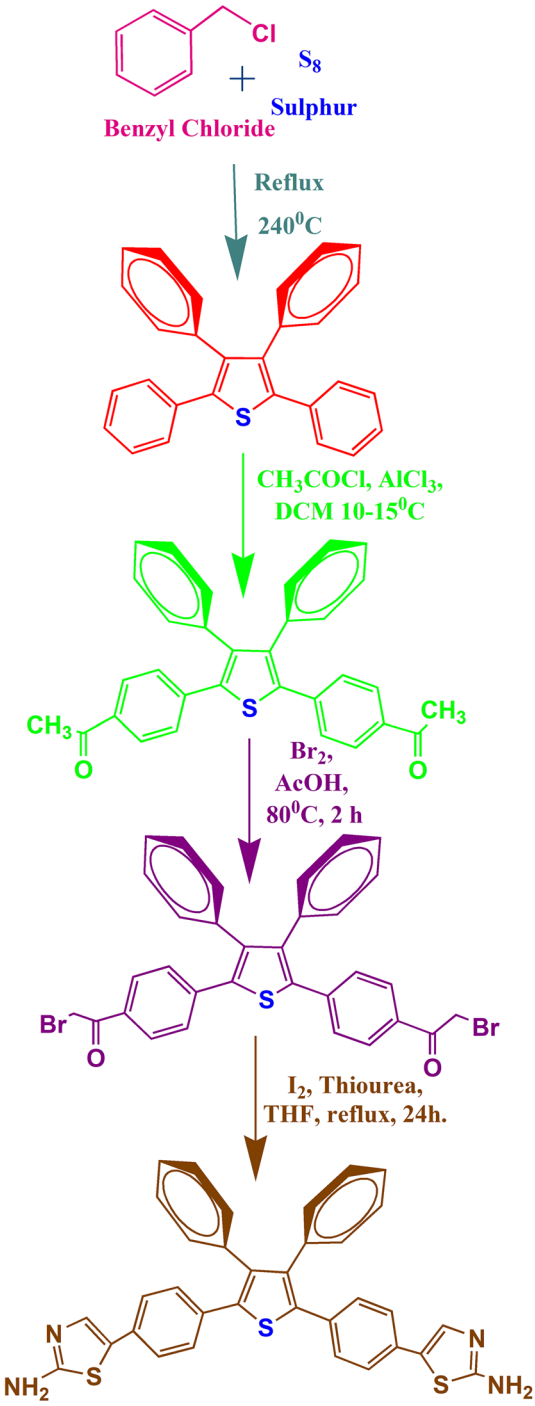

Scheme 1 Synthetic pathway for the synthesis of 2,5-bis(4-(2-aminothiazole) phenyl)-3,4-diphenyl thiophene diamine monomer (TPTPThDA)

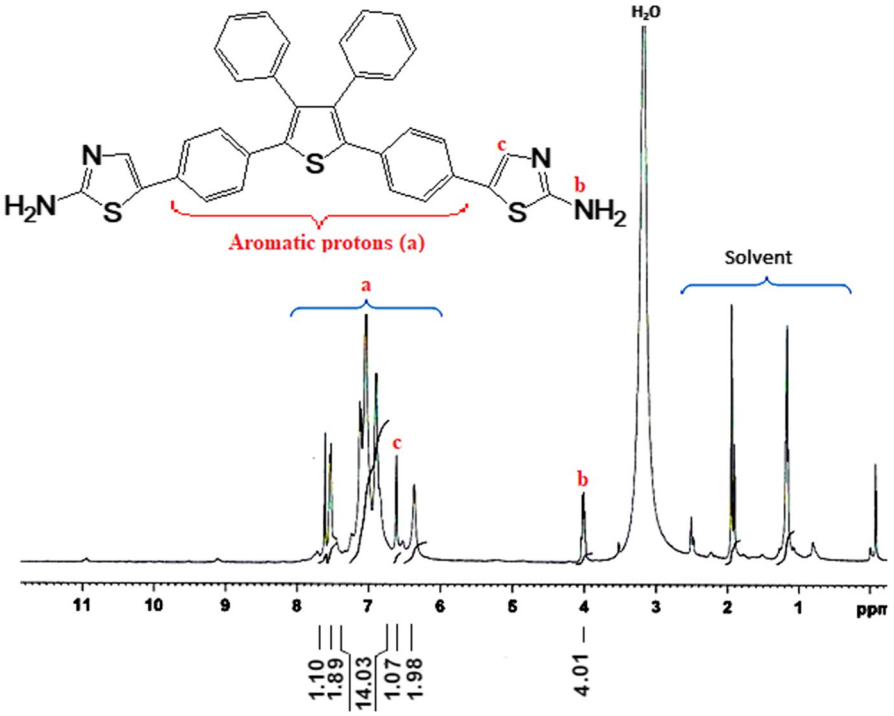

Fig. 1 [1]H-NMR spectra of TPTPThDA

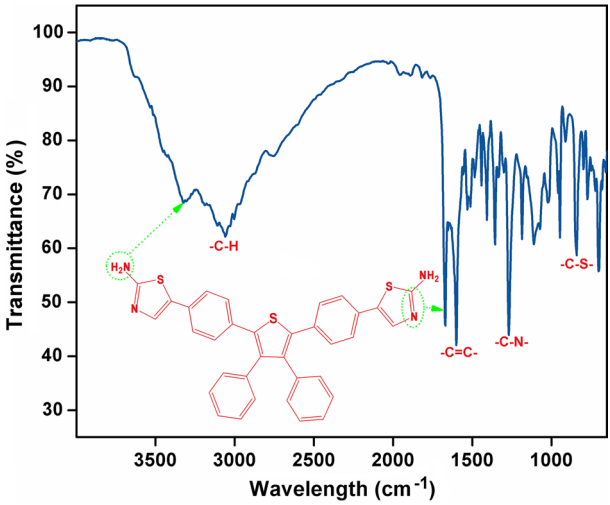

Fig. 2 FTIR spectrum of TPTPThDA

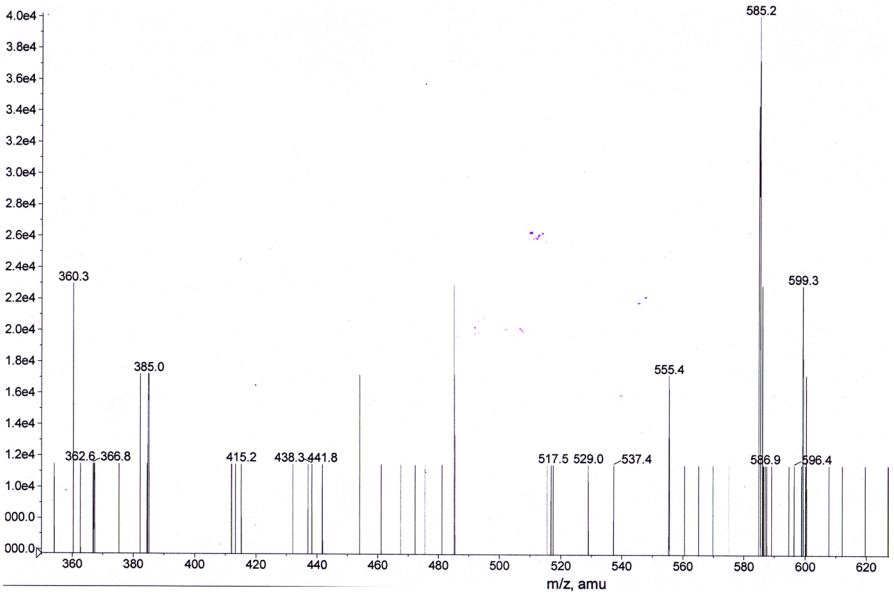

Fig. 3 MASS spectra of TPTPThDA

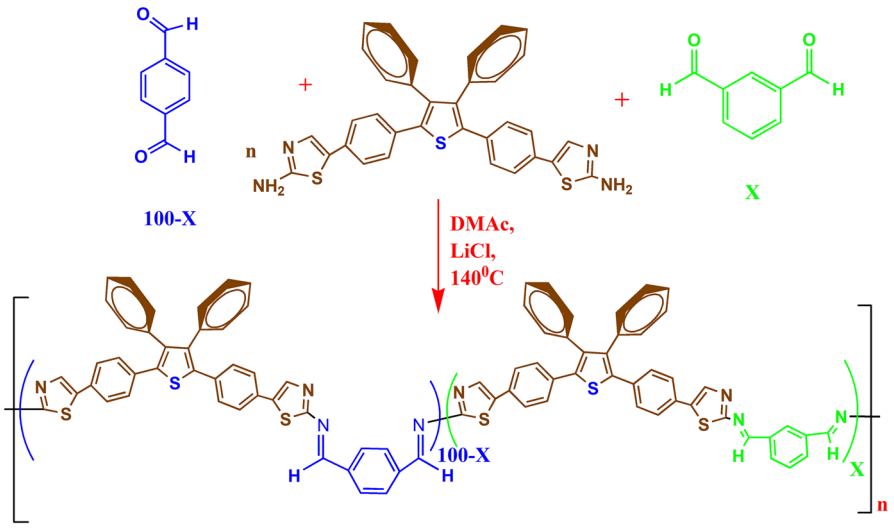

Scheme 2 Synthetic pathway for the synthesis of polyazomethines (PAM-01 to PAM-05)

The vibrational assignments of various thiophene–thiazole-based polymers are reported in Fig. 4. The stretching vibrations of –C=N– (azo linkages) absorption bands are typically located at 1598 cm^{-1}. The loss of stretching vibrations at 1700 and 3400–3150 cm^{-1} specified that total dialdehyde and diamine functionality had

Table 1 Synthesis of polyazomethines[a] from (TPTPThDA)

Polymer[a] code	Diamine mol %	Dialdehyde mol%		Yield (%)	Viscosity[b] η_{inh} (dL/g)
	TPTPThDA	TPA	IPA		
PAM-01	100	100	00	99	0.27
PAM-02	100	75	25	100	0.21
PAM-03	100	50	50	100	0.14
PAM-04	100	25	75	97	0.17
PAM-05	100	00	100	93	0.27

[a]Polymerization was carried out with 1 mmol each of diamine and dialdehyde

[b]Measured at a concentration of 0.5 g/dL in formic acid at 30 °C

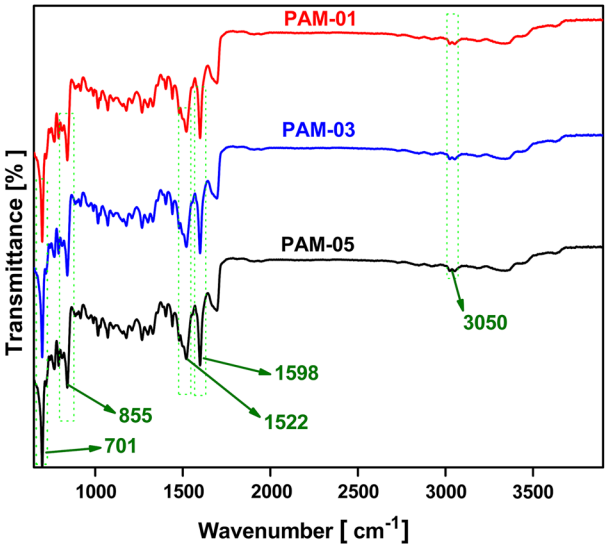

Fig. 4 IR spectra of PAMs

proceeded to produce with great molecular framework of PAMs. The stretching absorption at 1622 cm^{-1} is attributable to aromatic –C=C– stretching frequency of tetraphenylthiophene–thiazole unit which is well-constructed in polyazomethine [33]. The stretching at 3050 cm^{-1} explains the aromatic C-H moiety of the polyazomethines chain.

Solubility and inherent viscosity

As shown in Table 2, solubility of PAMs was proved qualitatively in numerous organic solvents. All PAMs were dissolved at room temperature in formic acid and conc.H_2SO_4. This is due to the fact that the polymers are containing more rigid structures, but are partly soluble in DMAc, DMSO, NMP and DMF. Moreover, they

Table 2 Solubility of polyazomethines (PAM-01 to PAM-05)

Polymers	Solvents								
	DMAc	DMF	NMP	DMSO	m-cresol	Conc. H_2SO_4	HCOOH	$CHCl_3$	DCM
PAM-01	+–	+–	+–	+–	+–	++	++	–	–
PAM-02	+–	+–	+–	+–	+–	++	++	–	–
PAM-03	+–	+–	+–	+–	+–	++	++	–	–
PAM-04	+–	+–	+–	+–	+–	++	++	–	–
PAM-05	+–	+–	+–	+–	+–	++	++	–	–

++, Soluble; +, soluble on heating; +–, partly soluble; –, insoluble

were totally insoluble in fewer active solvents such as dichloromethane and chloroform [31, 34, 35].

As shown in Table 1, the resulting PAMs hold inherent viscosities fluctuate commencing 0.14–0.28 dL/g, deliberated in formic acid at concentration of 0.50 dL/g at 30 °C.

XRD analysis

The X-ray diffraction (XRD) technique has been used to check the crystallinity/amorphous nature of series of polyazomethines (Fig. 5) over in the 2θ range of 5°–90° [36]. Broad diffraction peaks at ~ 12° and ~ 20° (2θ) were detected which support the amorphous nature of PAMs. No more sharp peaks are detected which specifies amorphous nature of PAMs. From the observed arrangements of PAMs, it

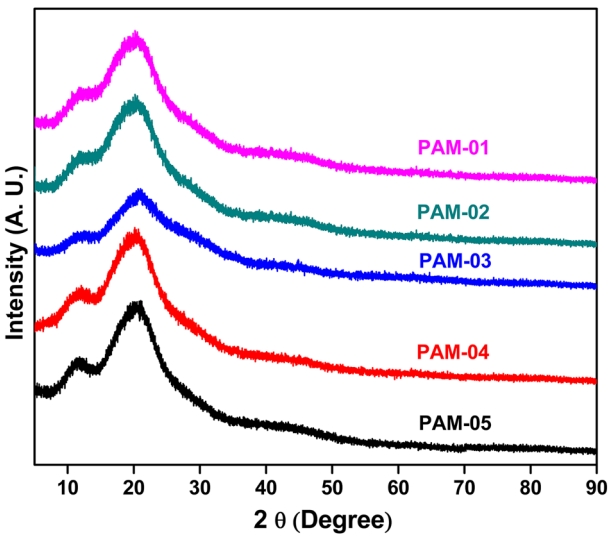

Fig. 5 XRD spectra of PAMs

is granted to confirm that considered material had an amorphous nature which was predicted and also in good compliance with the reported literature [37, 38].

Electrical conductivity measurement

Figure 6 deals with study of temperature dependence electrical conductivity of polyazomethines. The increase in the conductivity of PAMs as an activity of dialdehyde composition (IPA/TPA/IPA + TPA) is described in Fig. 6. Specifically, the conductivity increased when the dialdehyde (IPA) content was increased from 00 to 100 wt%. The conductivity result of PAMs films is 9.55×10^{-7} S/cm, 9.59×10^{-7} S/cm, 9.66×10^{-7} S/cm and 9.73×10^{-7} S/cm for PAM-01, PAM-02, PAM-04 and PAM-05, respectively, It is the highest for PAM-03 (50% IPA + 50%TPA), i.e. 9.93×10^{-7} S/cm. A further increase in conductivity credits to the successful replacement of 1,4 linkage (TPA) by 1,3 linkage (IPA) in the polyazomethine matrix. Polyazomethine films are of p-type semiconducting material.

UV–Visible analysis

The electronic status quo of the PAM-03 is defined in Fig. 7. Thin-film polymers were prepared in formic acid and spin-coated on the glass slides for UV–Vis measurements. PAM-03 showed two absorption bands in the UV–Vis spectra. The first absorption band at 254 is attributed to π–π* progression of aromatic ring conjugations. The next most important absorption area is sighted around 342 nm owing to n–π* transition of imine conjugations. From this, it was confirmed that all the precursors or starting material totally vanished and increased electron shifting in the polymer backbone. The polymers solution appeared dark

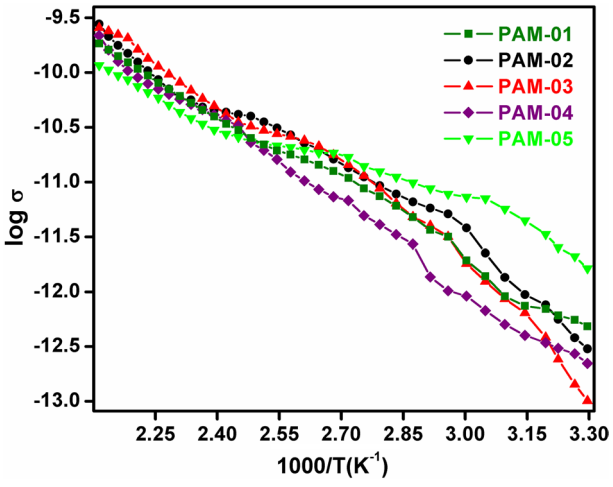

Fig. 6 Temperature dependence on electrical conductivity of polyazomethines (PAM-01 to PAM-05)

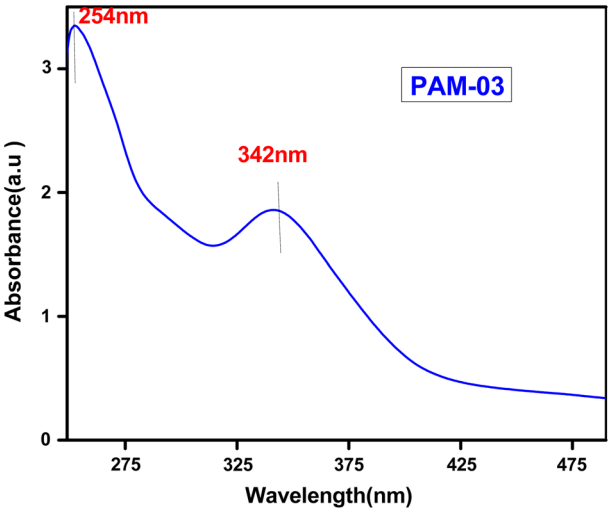

Fig. 7 UV–Vis spectra of PAM-03

Table 3 Absorption cut-off values λ max (nm) and energy band gap E_g (eV)

S. no.	Polymer	λ max (nm)	E_g (eV)
1.	PAM-03	342	3.63

yellow-orange to red, whereas the dialdehyde monomers appeared as colourless. Table 3 outlines the band gap energy (E_g) of PAM-03, and it is 3.63 eV [39].

In the conjugated systems, the electrons obstacle stuck between energy levels, that is prolonged pi orbitals, generated by a series of interchanging single and double bonds, frequently in aromatic systems. In addition, aromatic π-conjugated tetraphenyl with heterocyclic unit arrangements is energetic material composition which contains π–π intermolecular interrelations and it is advantageous for optical and electronic applications [40, 41]. This alteration is attributable to the interaction in the polyazomethines films, which upsurge the extent of orbital lap connecting the p electrons of the thiophene–thiazole ring units link with the lone pair of nitrogen atom in polyazomethines [42]. After polymerization of TPT-PThDA diamine monomer and dialdehyde monomers, there is prolonged conjugation of aromatic system with more unsaturated (multiple) bonds in a polymer backbone having a tendency to change in shift of absorption to corresponding wavelengths.

In whole, UV–visible spectroscopy data correlate with infrared spectra. They indicate the presence of imine linkages (1598 cm^{-1}) in polymer backbone, i.e. total conversion of primary amine to corresponding macromolecular-structured polyazomethines PAM-03.

Table 4 Thermal properties of polyazomethines (PAM-01 to PAM-05)

S. no.	Polymers	Thermal behaviour[a]				Residual wt% at 900 °C
		TGA in air		TGA in N_2		
		T_i	T_d	T_i	T_d	
1	PAM-01	211	458	217	550	63
2	PAM-02	219	545	270	601	65
3	PAM-03	202	528	262	588	58
4	PAM-04	203	466	261	587	60
5	PAM-05	214	476	240	527	62

T_d, temperature of 10% decomposition; T_i, initial decomposition temperature

[a]Temperature at which onset of decomposition was recorded by TG at a heating rate of 10 °C/min

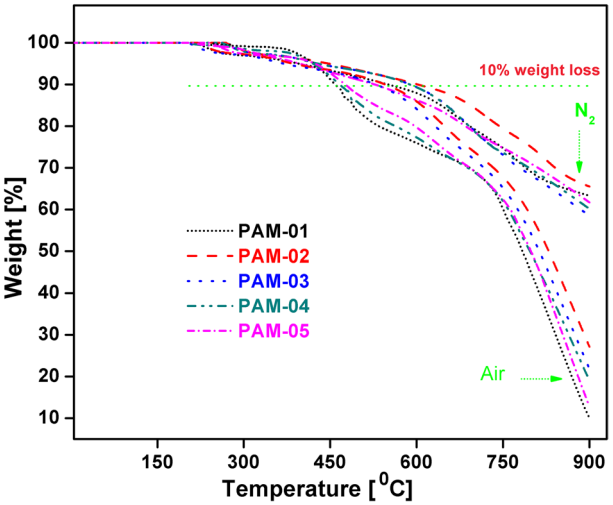

Fig. 8 TGA of polyazomethines in air and N_2

Thermal analysis

The thermal properties of the tetraphenylthiophene–thiazole-based PAMs were estimated by DSC and TGA (in both N_2 and air atmospheres). The outcomes are outlined in Table 4, and the representative TGA curves (in N_2 and in Air) of the polyazomethines are displayed in Fig. 8. As presented in Table 4, the strategy of polyazomethines with the merger of 1,4 and 1,3 linkages and bulky heteroaromatic tetraphenylthiophene–thiazole structure provides high thermal stability. Polymers PAM-01 to PAM-05 were stable up to the temperature around 458 °C in air and nitrogen atmosphere. The T_i of polyazomethines was in the range of 202–219 °C and 217–262 °C in nitrogen and air atmosphere, respectively. The temperatures at

10% weight loss were in the sort of 527–601 °C and 458–545 °C in nitrogen and air atmosphere, respectively. In addition, these polymers remained 58–65% and 10–27% of original weight at 900 °C in nitrogen and air atmosphere, respectively [31, 43–45]. Amongst these polyazomethines, the PAM-02 presented uppermost thermal stability with $T_{10\%}$ ca.601 °C in compliance with the previous reports [33, 36]. Polyazomethines composed of rigid backbone, i.e. para orientated (1,4 linkages, TPA) shows higher thermal stability than the meta orientated (1,3 linkages, IPA).This varying composition of polyazomethines (PAM-01 to PAAM-05) is also clearly seen in the residual weight at 900 °C [46, 47].

The heteroaromatic bulky polyazomethines give the glass transition temperature (T_g) in between 257 and 263 °C and are displayed in Fig. 8. The polymers PAM-01 and PAM-02 show the uppermost T_g value (262 °C) because of the presence of rigid 1,4-benzene linkage (TPA) and a lower ratio of 1,3 benzene linkage (IPA), whereas the polymer PAM-03 gave the lowest T_g value (257 °C) due to the existence of the heteroaromatic bulky unit and a equimolar ratio of 1,3 and 1,4 linkages [33]. The DSC arch for PAM-04 and PAM-05 reveals a T_g around at 260 °C (Fig. 9).

Morphology of PAM-03

Out of all the polyazomethines, PAM-03 shows good conductivity and it contains 50–50% (1,3 IPA and 1,4 TPA) in polymer chain (as shown in Fig. 6), and hence this was selected for morphology analysis. Figure 10a displays the scanning electron photomicrograph of PAM-03 thin film. The micrographs displaying large porosity with permeable granular analogous morphology are noticed for PAM-03 thin film. The permeable granular analogous morphology is beneficial for preoccupation of gases on exterior of thin film and could contribute a fine passageway for electron

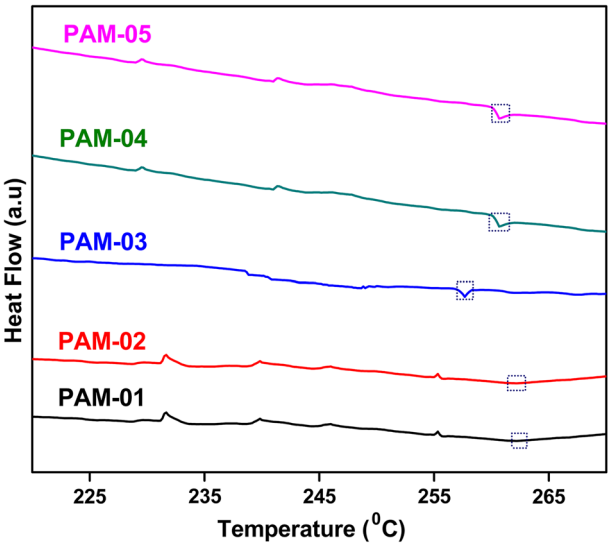

Fig. 9 DSC of polyazomethines (PAM-01 to PAM-05)

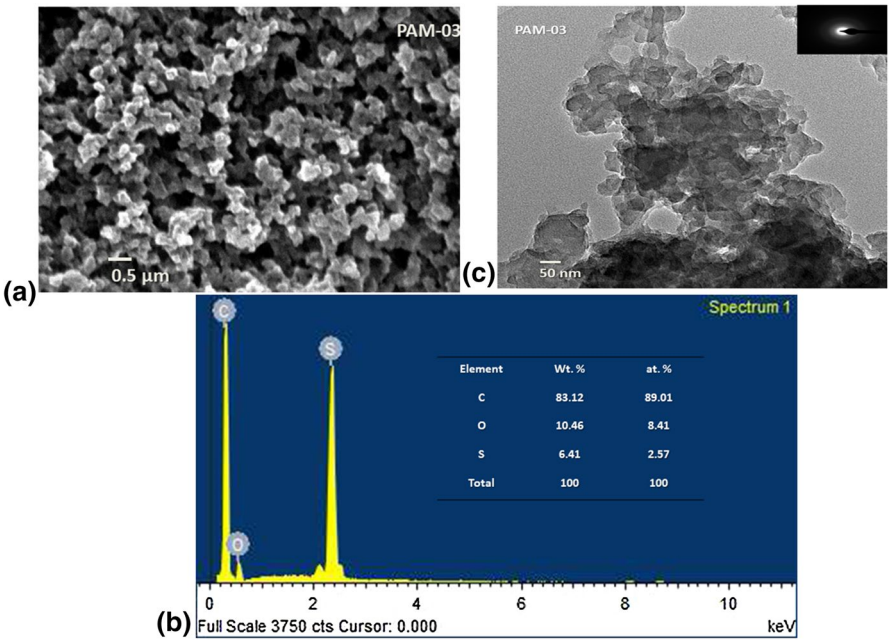

Fig. 10 **a** SEM image of PAM-03, **b** EDS of PAM-03 and **c** TEM image of PAM-03

relocation. Figure 10b shows EDS spectra of PAM-03 thin film. The EDS investigation showed the occurrence of sulphur, carbon and oxygen. The results support the coexistence of S, C and O elements in the pure organic polymeric sample of PAM-03 (as shown in Fig. 10b), and it indicated that high purified polyazomethines have been prepared by using solution polycondensation technique. Figure 10c displays transmission electron microscopy (TEM) image of PAM-03. The TEM image with particle size of 45–50 nm shows that polyazomethine matrix was homogeneously lengthened and moulded slack masses. It can be concluded from TEM images that nucleation of polyazomethines matrix manifests itself, and such type of nucleation sponsors preoccupation of gas molecules apparent over the PAM-03 thin film.

Gas sensing properties

Operating temperature for PAM-03 sensor

Gas response to maximum materials exclusively be contingent on operating temperature. The variation in the functioning temperature changes the rates of the surface assimilation and reaction taking place on the sensor exterior [48]. Consequently, the gas response was verified by various working temperatures (Fig. 11) and the operating temperature is set to 35 °C. Out of all polyazomethines, PAM-03 is showing good electrical conductivity (Fig. 6) and morphology (Fig. 10a), of which PAM-03 shows porous and granular, which is best for gas diffusion in polymer matrix and

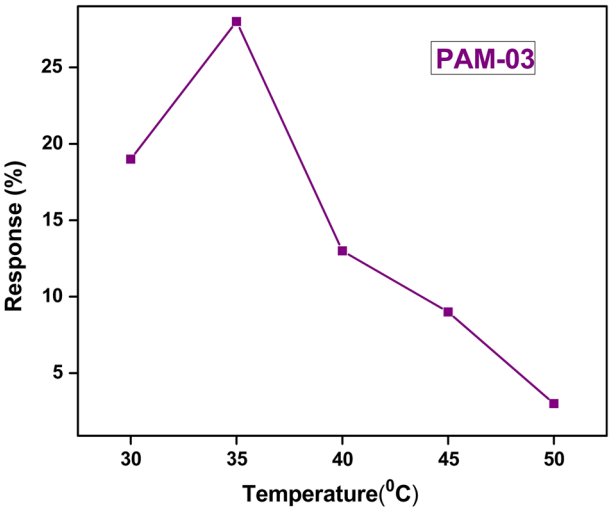

Fig. 11 Response of the PAM-03 sensors (100 ppm) at different operating temperatures

hence that was selected for gas sensing application. The challenging gas molecules prerequisite a convinced temperature towards beating the activation energy barricade towards respond with the exterior engrossed oxygen species. Equally the challenging gas molecules and the oxygen species demonstrated greater reaction action at 35 °C temperature and the sensor expressed developed greater response. Once the temperature is high, the trouble in gas surface assimilation grounds the reduced consumption speed of the detecting material, ensuing in the gas response dropping [49].

In this research work, various gas adsorptions were verified at optimal temperature, i.e. 35 °C. The outcomes are presented in Fig. 12. The sensor exhibited a

Fig. 12 Selectivity of PAM-03 towards various gases

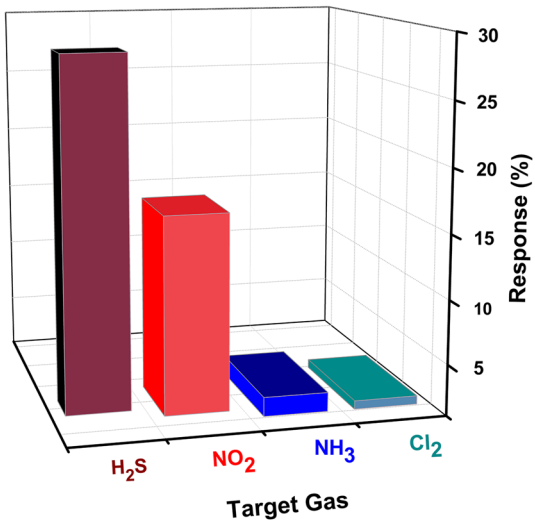

satisfactory response towards H_2S gas concentration of 100 ppm, and the response rises with an intensification in the H_2S concentration. An appreciated gas sensor should have mutually great sensitivity and decent selectivity. In command to selectivity of material to H_2S, 100 ppm of further gas molecules such as NH_3, NO_2 and Cl_2 was accommodated, hooked on trial method to extent their responses. The experimental outcomes are shown in Fig. 12. The outstanding selectivity can be attributed to the dissimilar reducibility between the challenging gases and their surface assimilation capability on the detecting material. In the gas detecting procedure, the engrossed H_2S molecules possibly form the metastable class (HSO–), prominent to the H_2S molecules that are simply oxidized by adsorbed oxygen species at 35 °C temperature matched with the other gas molecules.

As displayed in Fig. 13, the resistance curve of the sensor constructed on PAM-03 is enlarged after exposed in 100 ppm H_2S and recuperated towards the indecorous air level on coverage to air, which reveals the p-type semiconductor performance of PAM-03. The response rate of PAM-03 is expressively improved which may be affected by the huge surface capacity of material (as shown in Fig. 10a) for gas reoccupation and dispersion, fast transporter.

Selectivity of PAM-03 sensor

The capability of device towards reply in the direction of convinced gas in the attendance of alternative gases exists noted as selectivity. The selectivity of PAM-03 thin film was done underneath expose of altered gases H_2S, Cl_2, NH_3 and NO_2 at 35 °C. Figure 12 displays the gas response of PAM-03 thin film to dissimilar gases. PAM-03 thin film displays substantial selectivity towards H_2S gas and considerably weaker response to NO_2, NH_3 and Cl_2 gases. Additionally, it is perceived that PAM-03 thin films sense lesser concentration of H_2S with greater

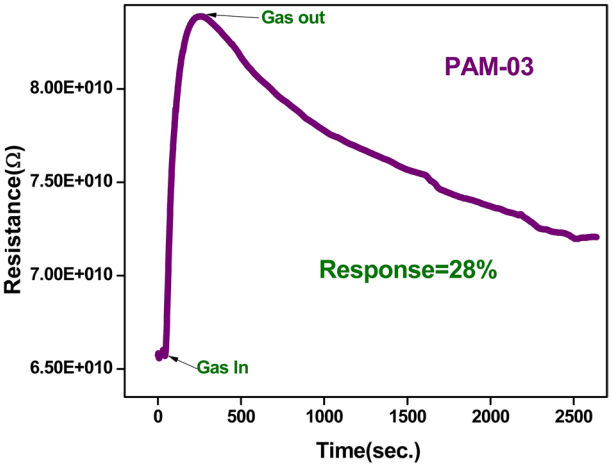

Fig. 13 Change in electrical resistance of PAM-03 sensor to H_2S (100 ppm) at 35 °C as a function of time

Table 5 Comparative response study of PAMs with previously reported materials towards H_2S gas

S. no.	Materials	Temperature	Gas type (concentration)	Response (%)	References
1.	α-Fe_2O_3 micro-ellipsoids	–	H_2S (100 ppm)	11.7	[50]
2.	Polythiophene-WO_3	–	H_2S (100 ppm)	13	[51]
3.	SnO_2/Ppy	RT	H_2S (100 ppm)	0.15	[52]
			H_2S (300 ppm)	0.42	
			H_2S (700 ppm)	0.68	
4.	CdS/PMMA	50 °C	H_2S (100 ppm)	15.9	[53]
		100 °C		23.7	
		150 °C		14.5	
5.	P3HT:Au-loaded ZnO nanoparticle	RT	H_2S (1000 ppm)	~1.3	[54]
6.	Poly(*N*-propylaniline) nanoparticles	RT	H_2S (100 ppm)	~20	[55]
7.	Polyaniline-polyethylene oxide	RT	H_2S (1 ppm)	5	[56]
8.	Ag-PPy, pTSA-Ag-PPy and Ppy	–	H_2S (50 ppm)	7.5	[57]
9.	Polyazomethines (PAM-03)	35 °C	H_2S (100 ppm)	28	Present work

sensitivity rate as related to higher absorptions of extra gases. The selectivity of PAM-03 thin film to sense H_2S gas is greater than that of different conducting polymers, and the results are summarized in Table 5 [50–57].

Gas sensing mechanism of PAM-03 sensor

The variation in the resistance of the PAM-03 sensor as a character of time is noted at 35 °C and presented in Fig. 13. It was found that, on disclosure of reducing H_2S gas on PAM-03 sensor, there was impulsive increase in the rate of resistance. Firstly, a polyazomethine sensor film is tolerable to acquire steady electrical resistance prior to bring H_2S gas, the steady electrical resistance is known as R_a (resistance in air), while the resistance of PAM-03 sensor in existence of target gas is known as R_g. We know that the polyazomethine is p-type material, since the dominance charge transporters are holes, further the H_2S gas is reducing in nature (electron donor). The interaction between polyazomethine film and exposed H_2S gas molecules causes raises in electric resistance values of PAM-03 film. When innovative resistance charge is attained, the H_2S gas had been offend and fresh air is instigated into the experiment compartment. The detected variation in the resistance of PAM-03 sensor with H_2S gas molecules is owed to the adsorption of gas on the exterior of PAM-03 sensor as well as the response for a specific gas or vapour is essentially correlated to surface accommodation rates of gas on active detecting sheet.

Conclusions

A series of PAMs were prepared by the high-temperature solution polycondensation of a novel diamine precursor 2,5-bis(4-(2-aminothiazole) phenyl)-3,4-diphenyl thiophene (TPTPThDA), with varying proportion of aromatic dialdehydes comonomer [1,3 linkage isophthalaldehyde (IPA) and 1,4 linkage terephthalaldehyde (TPA)]. Inherent viscosities of these PAMs were in between the 0.14 and 0.27 dL/g. These PAMs revealed soluble in HCOOH and conc.H_2SO_4. The temperature dependence dc electrical conductivity of PAM films was established in variety of 9.5×10^{-7} S/cm to 9.9×10^{-7} S/cm. The plot shows PAMs conductivity which covers the equimolar portion of [1,3 linkage isophthalaldehyde (IPA) and 1,4 linkage terephthalaldehyde (TPA)] in the polyazomethine films, which increases remarkably after insertion of 1,3 linkage means isophthalaldehyde (IPA) in the PAMs matrix. The existence of –C=N– (azo linkage) in the PAMs framework was committed by UV–Vis spectra. The H_2S gas-measuring sensor constructed on PAM-03 thin films was effectively developed by spin-coating method on a glass plate. The structure and morphological framework of the polyazomethine thin films is completed by SEM, TEM, XRD and FTIR methods. These films were originated to be extremely sensitive and selective towards H_2S gas working at 35 °C. Taking into explanation all the outcomes of gas detecting investigates, it is resolved that the PAM-03 sensor has decent detecting goods like selectivity to H_2S gas than further intrusive gases, greater gas response 28%. The enhanced gas detecting goods can be credited to extra adsorption spots delivered via the extra apertures and passages of the active thiophene–thiazole ring subunits. Moreover, the introduction of thiazole units to the mesoporous 1,2,3,4 tetraphenylthiophene (TPTP) cannot merely ease the detachment of engrossed oxygen; moreover, fast-track the dynamic exterior returns in H2S owing to the chemical sensibilise and extended conjugation of fine spread thiophene–thiazole ring subunits. These outcomes direct that the polyazomethine is established to be identical striking H_2S gas detecting sensible and has prospective application in the arena of gas sensors.

Acknowledgements The author gratefully acknowledges financial support from University Grants Commission, New Delhi, India Junior and Senior Research Fellowship (Y.S.P) in Science for CSIR-UGC NET.

References

1. Wetchakun K, Samerjai T, Tamaekong N, Liewhiran C, Siriwong C, Kruefu V, Wisitsoraat A, Tuantranont A, Phanichphant S (2011) Semiconducting metal oxides as sensors for environmentally hazardous gases. Sens Actuators B Chem 160:580–591
2. Santra S, Guha PK, Ali SZ, Hiralal P, Unalan H, Covington JA, Amaratunga G, Milne W, Gardner JW, Udrea F (2010) ZnO nanowires grown on SOI CMOS substrate for ethanol sensing. Sens Actuators B Chem 146:559–565
3. Hakim M, Broza YY, Barash O, Peled N, Phillips M, Amann A, Haick H (2012) Volatile organic compounds of lung cancer and possible biochemical pathways. Chem Rev 112:5949–5966

4. Shehada N, Brönstrup G, Funka K, Christiansen S, Leja M, Haick H (2015) Ultrasensitive silicon nanowire for real-world gas sensing: noninvasive diagnosis of cancer from breath volatolome. Nano Lett 15:1288–1295
5. Li X, Le TM, Dutta RK, Qiao S, Chandran GT, Penner RM (2017) Sub-6 nm palladium nanoparticles for faster, more sensitive H_2 detection using carbon nanotuber ropes. ACS Sens 2:282–289
6. Yadav AA, Kulkarni SB, Lokhande CD (2018) Synthesis and characterization of polypyrrole thin film by MW-CBD method for NH_3 gas sensor. Polym Bull. https://doi.org/10.1007/s00289-018-2282-5
7. Liu L, Zhang D, Zhang Q, Chen X, Xu G, Lu Y, Liu Q (2017) Smartphone-based sensing system using ZnO and graphene modified electrodes for VOCs detection. Biosens Bioelectron 93:94–101
8. Chandran GT, Li X, Ogata A, Penner RM (2016) Electrically transduced sensors based on nanomaterials (2012–2016). Anal Chem 89:249–275
9. Gerard M, Chaubey A, Malhotra B (2002) Application of conducting polymers to biosensors. Biosens Bioelectron 17:345–359
10. Janata J, Josowicz M (2003) Conducting polymers in electronic chemical sensors. Nat Mater 2:19
11. Shao F, Fan J, Hernández-Ramírez F, Fàbrega C, Andreu T, Cabot A, Prades J, López N, Udrea F, Luca AD (2016) NH_3 sensing with self-assembled ZnO-nanowire μHP sensors in isothermal and temperature-pulsed mode. Sens Actuators B Chem 226:110–117
12. Kaya İ, Çıtakoğlu N, Kolcu F (2017) Synthesis and characterization of semi conductive, thermally stable imine polymers containing methyl silane group. Polym Bull 74(4):1343–1369
13. Yang CJ, Jenekhe SA (1991) Conjugated aromatic poly(azomethines) characterization of structure, electronic spectra, and processing of thin films from soluble complexes. Chem Mater 3:878–887
14. Wang C, Shieh S, Legoff E, Kanatzidis MG (1996) Synthesis and characterization of a new conjugated aromatic poly (azomethine) derivative based on the 3′,4′-dibutyl-alfa- terthiophene buillding block. Macromolecules 29:3147–3156
15. Guarin SAP, Bourgeaux M, Dufresne S, Skene WG (2007) Photophysical, crystallographic, and electrochemical characterization of symmetric and unsymmetric self-assembled conjugated thiopheno azomethines. J Org Chem 72:2631–2643
16. Usluer Ö, Abbas M, Wantz G, Vignau L, Hirsch L, Grana E, Brochon C, Cloutet E, Hadziioannou G (2014) Metal residues in semiconducting polymers: impact on the performance of organic electronic devices. ACS Macro Lett 3:1134–1138
17. Urien M, Wantz G, Cloutet E, Hirsch L, Tardy P, Vignau L, Cramail H, Parneix JPP (2007) Field-effect transistors based on poly(3-hexylthiophene): effect of impurities. Org Electron Phys Mater Appl 8:727–734
18. Raut BT, Chougule MA, Ghanwat AA, Pawar RC, Lee CS, Patil VB (2012) Polyaniline–CdS nanocomposites: effect of camphor sulfonic acid doping on structural, microstructural, optical and electrical properties. J Mater Sci Mater Electron 23:2104–2109
19. Zayed MEM, Asiri AM, Khan SA (2016) Microwave assisted synthesis, spectrofluorometric characterization of azomethine as intermediate for transition metal complexes with biological application. J Fluoresc 26:937–947
20. Adams R, Bullock JE, Wilson WC (1923) Contribution to the structure of benzidine. J Am Chem Soc 45:521–527
21. Marvel CS, Hill HW (1950) Polyazines. J Am Chem Soc 72:4819–4820
22. Yang CJ, Jenekhe SA (1994) Effects of structure on refractive index of conjugated polyimines. Chem Mater 6:196–203
23. Yang CJ, Jenekhe SA (1995) Conjugated aromatic Polyimines. 2. Synthesis, structure, and properties of new aromatic polyazomethines. Macromolecules 28:1180–1196
24. Barik S, Bletzacker T, Skene WG (2012) π-Conjugated fluorescent azomethine copolymers: optoelectronic, halochromic, and doping properties. Macromolecules 45:1165–1173
25. Barik S, Friedland S, Skene WG (2010) Understanding the reversible anodic behaviour and fluorescence properties of fluorenylazomethines—A structure–property study. Can J Chem 88:945–953
26. Das M, Sarkar D (2018) Development of room temperature ethanol sensor from polypyrrole (PPy) embedded in polyvinyl alcohol (PVA) matrix. Polym Bull 75:3109
27. Barik S, Skene WG (2013) Turning-on the quenched fluorescence of azomethines through structural modifications. Eur J Org Chem 2013:2563–2572
28. Iwan A, Palewicz M, Chuchmała A, Gorecki L, Sikora A, Mazurek B, Pasciak G (2012) Opto(electrical) properties of new aromatic polyazomethines with fluorene moieties in the main chain for polymeric photovoltaic devices. Synth Met 162:143–153

29. Tsai FC, Chang C, Liu C, Chen WC, Jenekhe SA (2005) New thiophene-linked conjugated poly (azomethine)s: theoretical electronic structure, synthesis, and properties. Macromolecules 38:1958–1966
30. Aly KI, Abbady MA, Mahgoub SA, Hussein MA (2007) Liquid crystalline polymers IX main chain thermotropic poly (azomethine—ether)s containing thiazole moiety linked with polymethylene spacers. Express Polym Lett 1:197–207
31. Imai Y, Maldar NN, Kakimoto MA (1984) Synthesis and characterization of soluble aromatic polyazomethines from 2,5-bis(4-aminophenyl)-3,4-diphenylthiophene and aromatic dialdehydes. J Polym Sci Part A Polym Chem 22:3771–3778
32. Ubale VP, Sagar AD, Maldar NN, Birajdar MV (2001) Synthesis and characterization of aromatic–aliphatic polyamides. J Appl Polym Sci 79:566–571
33. Ankushrao SS, Patil YS, Ubale VP, Maldar NN, Ghanwat AA (2017) Synthesis and characterization of thermally stable poly(ether-azomethine)s derived from 1,1-bis[4-(4-benzaldehyde oxy)-3-methyl phenyl] cyclopentane. J Macromol Sci Part A 54:411–417
34. Hsiao SH, Liou GS (2002) A new class of aromatic poly(1,3,4-oxadiazole)s and poly(amide-1,3,4-oxadiazole)s containing (naphthalenedioxy)diphenylene groups. Polym J 34:917–924
35. Patra S, Lenka S, Nayak PL (1986) Synthetic resins II. Preparation and characterization of resins prepared from aminoacetophenone. J Appl Polym Sci 32:5071–5083
36. Ankushrao SS, Kadam VN, Patil YS, Ubale VP, Maldar NN, Ghanwat AA (2017) Synthesis and characterization of processable heat resistant co-poly(ester-amide)s containing cyclopentylidene moiety. J Macromol Sci Part A 54:124–132
37. Niu H, Huang Y, Bai X, Li X, Zhang G (2004) Study on crystallization, thermal stability and hole transport properties of conjugated polyazomethine materials containing 4,4′-bisamine-triphenylamine. Mater Chem Phys 86:33–37
38. Jarzabek B, Weszka J, Domanski M, Jurusik J, Cisowski J (2008) Optical studies of aromatic polyazomethine thin films. J Non Cryst Sol 354:856–862
39. Mahindrakar JN, Patil YS, Salunkhe PH, Ankushrao SS, Kadam VN, Ubale VP, Ghanwat AA (2018) Optically transparent, organosoluble poly(ether-amide)s bearing triptycene unit; synthesis and characterization. J Macromol Sci Part A 55(9):658–667
40. Salunkhe PH, Patil YS, Patil VB, Navale YH, Ubale VP, Dhole IA, Maldar NN, Ghanwat AA (2018) Synthesis and characterization of conjugated porous polyazomethines with excellent electrochemical energy storage performance. J Polym Res 25(7):147
41. Patil YS, Salunkhe PH, Navale YH, Ubale VP, Patil VB, Maldar NN, Ghanwat AA (2018) Synthesis, characterization and conductivity study of co-polyazomethine polymer containing thiazole active ring. AIP Conf Proc 1989:020034
42. Bochenkov VE, Sergeev GB (2005) Preparation and chemiresistive properties of nanostructured materials. Adv Colloid Interface Sci 116:245–254
43. Bera D, Padmanabhan V, Banerjee S (2015) Highly gas permeable polyamides based on substituted triphenylamine. Macromolecules 48:4541–4554
44. Salunkhe PH, Ankushrao SS, Patil YS, Mahidrakar JN, Kadam VN, Ubale VP, Ghanwat AA (2018) Processable heat resistant polyamides containing tetraphenyl thiophene having pendant phenyl moiety with heterocyclic quinoxaline unit: synthesis and characterization. J Macromol Sci Part A 55(4):377–383
45. Patil YS, Mahindrakar JN, Salunkhe PH, Ubale VP, Ghanwat AA (2018) Synthesis, characterization and structure–property relationships of processable poly(amide-imide)s containing novel tetraphenylthiophene–thiazole diimide-diacid (TPTPThDIDA) moiety. J Macromol Sci Part A 55(7):572–581
46. Patil YS, Salunkhe PH, Mahindrakar JN, Ankushrao SS, Kadam VN, Ubale VP, Ghanwat AA (2019) Synthesis and characterization of aromatic polyimides containing tetraphenylfuran-thiazole moiety. J Therm Anal Calorim 135(6):3057–3068
47. Salunkhe PH, Patil YS, Kadam VN, Mahindrakar JN, Ubale VP, Ghanwat AA (2019) Synthesis and characterization of processable polyamides containing polar quinoxaline unit in the main chain and evaluation of its hydrophilicity. J Macromol Sci Part A. https://doi.org/10.1080/10601325.2019.1569469
48. Chougule MA, Pawar SG, Godse PR, Mulik RN, Sen S, Patil VB (2011) Synthesis and characterization of polypyrrole (PPy) thin films. Soft Nanosci Lett 1:6–10
49. Chougule MA, Sen S, Patil VB (2012) Development of nanostructured polypyrrole (PPy) thin film sensor for NO_2 detection. Sens Transducers J 139:122–132

50. Li ZJ, Lin ZJ, Wang NN, Huang YW, Wang JQ, Liu W, Fu YQ, Wang ZG (2016) Facile synthesis of α-Fe_2O_3 micro-ellipsoids by surfactant-free hydrothermal method for sub ppm level H_2S detection. Mater Des 110:532–539
51. Bai S, Zhang K, Sun J, Zhang D, Luo R, Li D, Liu C (2014) Polythiophene-WO_3 hybrid architectures for low-temperature H_2S detection. Sens Actuators B 197:142–148
52. Waghuley SA (2011) Tin dioxide/polypyrrole multilayer chemiresistor as a hydrogen sulfide gas sensor. J Electron Devices 10:433–437
53. Iftikhar MA, Awattif AM (2017) CdS/PMMA based inorganic/organic heterojunction for H_2S gas sensing. Chalcogenide Lett 14(4):133–138
54. Kruefu V, Wisitsoraat A, Tuantranont A, Phanichphant S (2014) Gas sensing properties of conducting polymer/Au-loaded ZnO nanoparticle composite materials at room temperature. Nanoscale Res Lett 9:467
55. Chabukswar VV, Bhavsar SV, Horne AS, Handore K, Gaikwad VB, Mohite KC (2013) Conducting poly(N-propylaniline) nanoparticles for hydrogen sulfide gas detection. Macromol Symp 327:39–44
56. Mousavi S, Kang K, Park J, Park I (2016) A room temperature hydrogen sulfide gas sensor based on electrospun polyaniline polyethylene oxide nanofibers directly written on flexible substrates. RSC Adv 6:104131
57. Karmakar N, Fernandes R, Jain S, Patil UV, Shimpi NG, Bhat NV, Kothari DC (2017) Room temperature NO_2 gas sensing properties of p-toluenesulfonic acid doped silver-polypyrrole nanocomposites. Sens Actuators B 242:118–126

Publisher's Note Springer Nature remains neutral with regard to jurisdictional claims in published maps and institutional affiliations.